JMEPEG
https://doi.org/10.1007/s11665-024-09473-9

1059-9495/$19.00

ORIGINAL RESEARCH ARTICLE

Development of a Novel β-Type Zr-25Ta-5Ti Alloy

Edriely de Oliveira Saraiva, Gerson Santos de Almeida, Willian Fernando Zambuzzi, and Pedro Akira Bazaglia Kuroda, and Carlos Roberto Grandini

Submitted: 18 August 2023 / Revised: 13 February 2024 / Accepted: 10 March 2024

This study aims to produce a novel zirconium alloy containing 25 wt.% tantalum and 5 wt.% titanium (Zr-25Ta-5Ti) as a biomaterial. The proposed Zr-25Ta-5Ti was prepared in an arc-melting furnace and subjected to annealing heat treatment at 1000 °C for 24 h to homogenize the microstructure and relieve residual melting stresses. After annealing, the alloy was submitted by hot-rolled process conformation to produce regular material. Chemical composition analyses show that the Zr-25Ta-5Ti alloy has good quality and homogeneity. The homogenization heat treatment increased the density of the Zr-25Ta-5Ti alloy (7.6 → 7.8 g/cm^3) due to the formation of the α phase. Structural and microstructure characterization data showed that the Zr-25Ta-5Ti alloy has α, β, and ω phases as a crystalline structure, where the homogenization heat treatment promoted the segregation of the Ta element at the grain boundaries of the β structure, and as a consequence, promoted the formation of the α phase. The hardness of the alloy is superior to titanium and zirconium elements (499 ± 5 HV for as-cast condition and 272 ± 7 HV for the annealed condition). Finally, the Zr-25Ta-5Ti alloy has low values of elastic modulus (86 ± 5 GPa for hot-rolled alloy) compared to commercial metallic biomaterials and biological tests indicated that alloys are not cytotoxic. Thus, taken the data together, this study brings Zr-25Ta-5Ti as a novel biomaterial to be used in biomedical applications.

Keywords biocompatibility, biomaterials, bone, cell, cytotoxicity, zirconium alloys

1. Introduction

The use of implants has grown significantly over the last years, driven by the aging of the world population, which brings with it the increase in diseases due to skeletal dysfunctions resulting from the natural wear and tear of the human body. In this sense, the demand for novel biomedical materials has been increased in dental and medical fields (Ref 1). Some of the expected properties of materials include the hardness, tensile strength, elastic modulus, and biocompatibility. It is known that a metallic implant used in the orthopedic area should have mechanical compatibility with the human bone to avoid a possible failure of the implant (Ref 2). The implanted material is expected to develop a natural elastic modulus value similar to bone. The bone elasticity modulus values range from 4 to 30 GPa, depending on the bone type, location, and measurement direction (Ref 3).

The mostly used metallic materials as biomaterials (CP-Ti, titanium alloys, Co-Cr alloys, and stainless steel) develop a greater elastic modulus than cortical bone; as a consequence, the implants absorb the load necessary for the bone to maintain its bone density, resulting in the loss of bone density over time, loosening the implant, and requiring revision surgery in the patient (Ref 4). This mechanical incompatibility leads to the death of bone cells and it is termed "stress shielding" (Ref 5). Thus, a material with excellent combination, high strength, and low elastic modulus should be the most indicated to be used as a biomaterial (Ref 6).

The most widely used titanium alloy in biomedical applications is still the Ti-6Al-4 V (Ref 7), with biocompatibility and biological responses already described within the literature (Ref 8). However, there are reports showing the cytotoxicity of vanadium, while aluminum has been associated with neurological disorders (Ref 9). To better work on this matter, new alloys without these elements are being proposed (Ref 2).

Zirconium has chemical and physical properties like titanium and has an allotropic transformation at a temperature of 862 °C (Ref 10). Adding this element into titanium alloys causes increased corrosion resistance, improved biocompatibility (Ref 11, 12), and decreases the melting point of alloys with refractory elements (Ref 13, 14).

Tantalum has been widely used as a biomaterial due to its excellent biocompatibility and corrosion resistance. However, Ta has poor wear resistance, which limits its application in load-bearing implants. Ta-Zr alloys have been developed to overcome this limitation, and results show great potential for biomedical applications due to high wear resistance and good mechanical properties (Ref 3). The Ta-15Zr alloy exhibited higher hardness and better wear resistance than pure-Ta in this system. These findings suggest that Ta-Zr alloys may be promising materials for load-bearing implants such as joint replacements (Ref 15).

Thus, this study aims to produce and characterize a novel zirconium alloy containing 5 wt.% titanium and 25 wt.%

Edriely de Oliveira Saraiva and **Carlos Roberto Grandini**, Laboratório de Anelasticidade e Biomaterials, UNESP–University Estadual Paulista, Bauru, São Paulo 17.033-360, Brazil; **Gerson Santos de Almeida** and **Willian Fernando Zambuzzi**, Laboratório de Bioensaios e Dinâmica Celular, UNESP–University Estadual Paulista, Botucatu, São Paulo 18618-970, Brazil; and **Pedro Akira Bazaglia Kuroda**, Materials Engineering Department (DEMa), UFSCar–University Federal de São Carlos, São Carlos, São Paulo 13.565-905, Brazil. Contact e-mail: pedro.kuroda@ufscar.br.

Published online: 24 April 2024

tantalum (Zr-25Ta-5Ti) through thermomechanical treatments, aiming to achieve the well-defined properties for a material being considered for biomedical applications.

2. Materials and Methods

The pure materials were weighed according to alloy stoichiometry and cleaned using the standard procedure for this type of material (Ref 16). The Zr (99.8% purity, Aldrich), Ta (99.9% purity, Good Fellow), and Ti (99.8% purity, Sandinox) elements were melted using an arc-voltaic furnace, with a water-cooled copper crucible with cylindric format, non-consumable tungsten electrode, and controlled argon atmosphere to avoid contamination (Ref 17, 18). The melting process of Ti, Ta, and Zr was repeated ten times due to the high melting point of Ta.

An annealing heat treatment was performed to reduce regions of micro-segregation of the Zr, Ta, and Ti elements. Atoms diffuse into regions of nonuniform composition when the time and temperature are high enough for this to occur. The annealing heat treatment performed in this study involved raising the temperature to 1000 °C at low pressure (10^{-7} Torr), with a heating rate of 10 °C/min, maintaining this temperature for 24 hours, and then slowly cooling the sample. The hot-rolling process was carried out using a FENN machine. The sample was held at approximately 1000 °C during the rolling process. Reheating the samples for 5 minutes occurred every three passes and then cooled in air. The final thickness of the sample was approximately 4 mm.

The chemical characterization of the Zr-25Ta-5Ti alloy was performed through density measurements, using the Archimedes method, on a precision balance (Ohaus, Explorer model − 0.0001 g accuracy). The sample's chemical composition was analyzed using the energy dispersion spectrometry (EDS) technique, which consists of the semi-quantitative detection of the elements present in the Zr-25Ta-5Ti alloy. The measurements were performed in an Oxford equipment, Prisma model, coupled to a Carl Zeiss scanning electron microscope (SEM) model EVO-LS15.

The structural characterization of the Zr-25Ta-5Ti alloy was made using x-ray diffraction, using a Rigaku diffractometer, MiniFlex600 model, with Cu Kα radiation (λ = 1.54056 Å). The data were collected using the powder method and the fixed-time mode, with steps of 0.04°, ranging from 20° to 100°, with 2θ step and 10°/min. The microstructural characterization of the samples was obtained using the Olympus optical microscope model BX51M (OM) and the Carl Zeiss scanning electron microscope model EVO-15 (SEM).

The initial mechanical characterization was performed from the hardness analysis performed in a Shimadzu microdurometer model HMV-2. The samples were indented five times in different regions. A force of 0.245 N, with 25 g and a duration of 60 s, was used. The technical standards for this test were followed (Ref 14, 15). For elastic modulus measurements, Sonelastic equipment from ATCP Engenharia Física was used. The measurements were based on the impulse excitation technique, following the ASTM E1876-15 standard (Ref 19).

Steel balls (AISI 52100) with a diameter of 25.4 mm and a hardness of 818 HV were used to conduct micro-abrasive wear tests in a dry environment. The balls rotated at 200 revolutions per minute (rpm) for 60 minutes, resulting in wear craters in the Zr-25Ta-5Ti alloy. It applied a 200 g load for these tests. The wear volume (V) and wear coefficient (K) was calculated using Archard's law (Ref 20). The parameters established for the wear tests were chosen according to previous studies (Ref 21).

Finally, biological characterization was done by managing cell viability and adhesion assays using pre-osteoblastic cells (MC3T3-E1, subclone 4). Previously, the materials were used to conditionate the cell culture medium which was further used to treat the cells up to 24 hours, following the recommendation of ISO:10993-5 (Ref 16). Thereafter, the conditioned medium was supplemented with 10% Fetal Bovine Serum (FBS) and properly used to challenge pre-osteoblasts for 24 h; viability was measured by the indirect cytotoxicity test (MTT), adding 1 mg/mL thiazolyl blue tetrazolium bromide salt (Sigma-Aldrich #M5455-1G) to the culture medium, placed in an CO_2 incubator for an additional 3 hours (Ref 22, 23). DMSO was used to solubilize the dye formed by viable cells. Absorbance was measured at 570 nm with SYNERGY-HTX multi-mode reader (Biotek, USA).

The pre-osteoblasts were treated for 24 h and later trypsinized and reseeded in order to evaluate the impact of the biomaterial on adhesion of cells (Ref 24). Adherent cells were washed in PBS and fixed in ethanol-absolute glacial acetic acid (3:1, v/v) for 10 minutes. Adherent cells were stained with 0.1% crystal violet (w/v) for 10 minutes; excess dye was properly removed, and the dye extracted to measure the absorbance at 540 nm (Ref 25, 26).

The GraphPad Prism 7 software (GraphPad Software, USA) was used for variance analysis (unpaired t test) or nonparametric analysis. The p value < 0.05 was considered statistically significant.

3. Results and Discussion

Figure 1 shows the chemical composition via EDS, where well-defined peaks of the Kα and Mα energies of zirconium, tantalum, and titanium elements were found. No energy peaks of other elements considered traces were detected, indicating the high-purity of this formulation.

Through the semi-quantitative analysis of EDS, Zr (blue), Ta (green), and Ti (red) elements were mapped to verify the

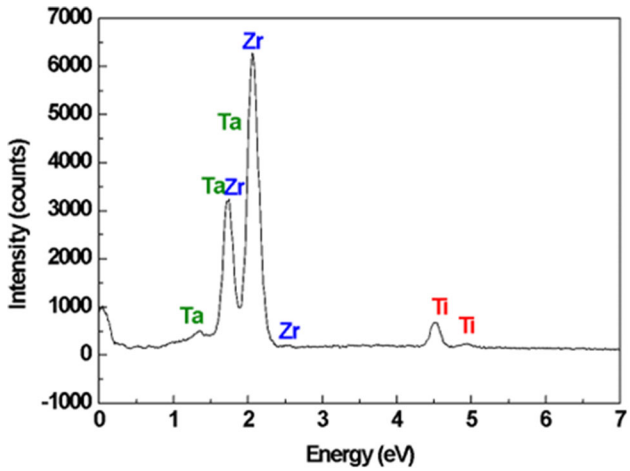

Fig. 1 Energy dispersive spectroscopy for a sample of as-cast Zr-25Ta-5Ti alloy

homogeneity and stoichiometry of the produced alloys (Fig. 2), showing purity and homogeneity in the produced alloy, which corroborates with the analysis of Fig. 1. The chemical composition results via EDS are presented in Fig. 1 legend, showing that the produced alloy has a chemical composition like the nominal values. The ASTM standard for the Ti-15Mo alloy suggests that the error in the weight percentage of molybdenum for a produced alloy should be less than 1% (Ref 27). Thus, an alloy with 14 and 16% weight of molybdenum can be considered satisfactory and designated as Ti-15Mo. Extrapolating the standard to the Zr-25Ta-5Ti alloy, the variation, plus or minus, of the amount of Zr should be 1.7% in weight of the alloy (23.3–26.7), and the error for Ti should be less than 0.3% (4.7–5.3).

Considering these data, it can be concluded that the variation of Zr was well below the standard, the variation of Ta is within the expected range, and there was no variation in Ti, resulting from a adequate melting process.

Additionally, density analysis was performed using the Archimedes principle. Understanding the density of a metal considered a biomaterial has been analyzed in the scientific community because metals have a high-density value compared to human cortical bone, and metals implanted with high density increase the load applied to repaired bone tissue. In this regard, titanium alloys that contain aluminum, such as Ti-6Al-4 V, have a physical advantage because substituting aluminum reduces the density of titanium alloys (Ref 28). On the other hand, the toxicity of Al due to the release of ions into the bloodstream has been proven (Ref 29), however, a better discussion and definition about the physiological concentration of Al needs to be better addressed.

The produced alloy has a density of 7.6 ± 0.1 g/cm^3, similar to the theoretical value one (7.7 g/cm^3), indicating that stoichiometry was respected; after the annealing treatment, it was observed that the density of the alloys increased (7.8 ± 0.4 g/cm^3), while after hot-rolling, the value showed a noticeable decrease (7.1 ± 0.3 g/cm^3).

The heat treatment with slow cooling (annealing) promotes the formation of the α phase (hexagonal close-packed structure), which is stable at low temperatures (Ref 30), and the α phase has a higher atomic packing factor than the β phase, making it denser (Ref 31). As a result, there was a slight increase in density in the alloy subjected to the heat treatment. After hot-rolling, there was a decrease in the density value, indicating a probable increase in the β phase and a reduction in the α phase. The β phase has a lower packing factor, hence less dense. The results of microstructural characterization will clarify the statements regarding the density values.

The average density of human cortical bone is approximately 1.5 g/cm^3. Alloys such as Ti-6Al-4 V, Ti-15Mo, TNZT, Co-Cr, and stainless steel are commonly used as biomaterials has a density from 4.4 g/cm^3 (Ti-6L-4 V) to 8.9 g/cm^3 (Co-Cr) (Ref 32). Comparing these alloys with the produced Zr-25Ta-5Ti alloy, its density (7.6 ± 0.1 g/cm^3 in as-cast condition) is a good value, suggesting that the Zr-25Ta-5Ti alloy may be a promising option as a biomaterial due to its high compatibility with human bone and its potential ability to support mechanical loads.

An empirical theory for determining the phases of alloys has been developed (Ref 33). To calculate the α and β phases, two elements, aluminum, and molybdenum, were chosen as references for phase stabilization, respectively (Ref 34). Equations 1 and 2 are shown below, representing the equivalence of Al (Al-eq) for predicting the α phase and the equivalence of Mo (Mo-eq) for predicting the β phase.

To better understand the phase predicted by the theory for the Zr-25Ta-5Ti alloy, the values of Mo-eq and Al-eq were plotted on the diagram (Fig. 3), adapted from John Mantione et al. 2020 (Ref 35). From the diagram, it can be observed that the Zr-25Ta-Ti alloy is located in a region rich in α phase, but small amounts of α' (distorted hexagonal close-packed) and β phases may be detected. Therefore, heat treatments or mechanical deformations may alter the quantities of phases present in the Zr-25Ta-5Ti alloy.

$$[\mathrm{Mo}]\mathrm{eq} = \mathrm{Mo} + 0.28\mathrm{Nb} + 0.22\mathrm{Ta} + 0,67\mathrm{V} + 1.60\mathrm{Cr} \quad \text{(Eq 1)}$$

$$[\mathrm{Al}]\mathrm{eq} = \mathrm{Mo} + 0.17\mathrm{Zr} + 0.33\mathrm{SnTa} + 10.0.O \quad \text{(Eq 2)}$$

Thermo-Calc is a widely used computational simulation software in the metallurgical and materials industry to predict and optimize the behavior of metallic alloys under different processing conditions (Ref 36). The program was used to understand how crystalline phases change as a function of temperature based on thermodynamic and phase equilibrium calculations, allowing for the prediction of microstructures, mechanical properties, etc. Considering Fig. 4, it was possible to observe the suppression of the α phase with increasing temperature and the β phase precipitation, where the β transus is at 647 °C, and the liquidus is at 2077 °C. It is worth noting that the annealing heat treatment and hot-rolling were performed above the β transus temperature, that is, in the β region.

Figure 5 shows the x-ray diffraction patterns obtained for pure Zr, Ta, Ti, and the Zr-25Ta-5Ti alloys after melting, annealing, and hot-rolling. The Zr-25Ta-5Ti as-cast condition alloy presents a structure consisting of hexagonal close-packed

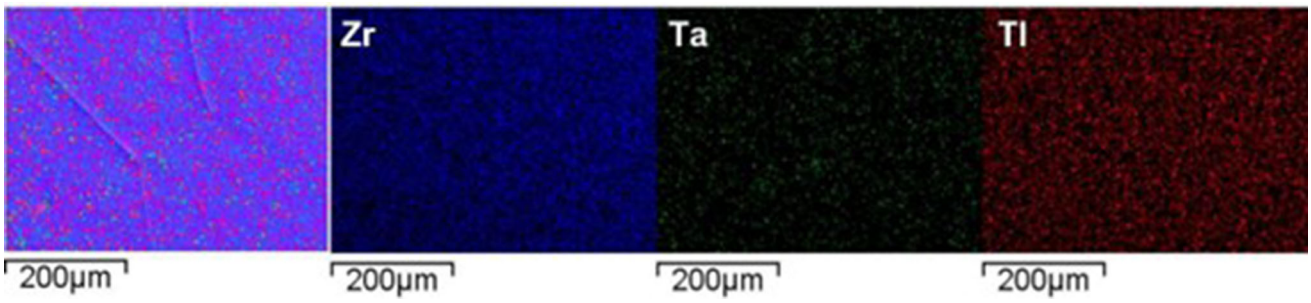

Fig. 2 EDS elemental mapping of as-cast Zr-25Ta-5Ti alloy (Zr = 68%, Ta = 27% and Ti = 5 wt.%)

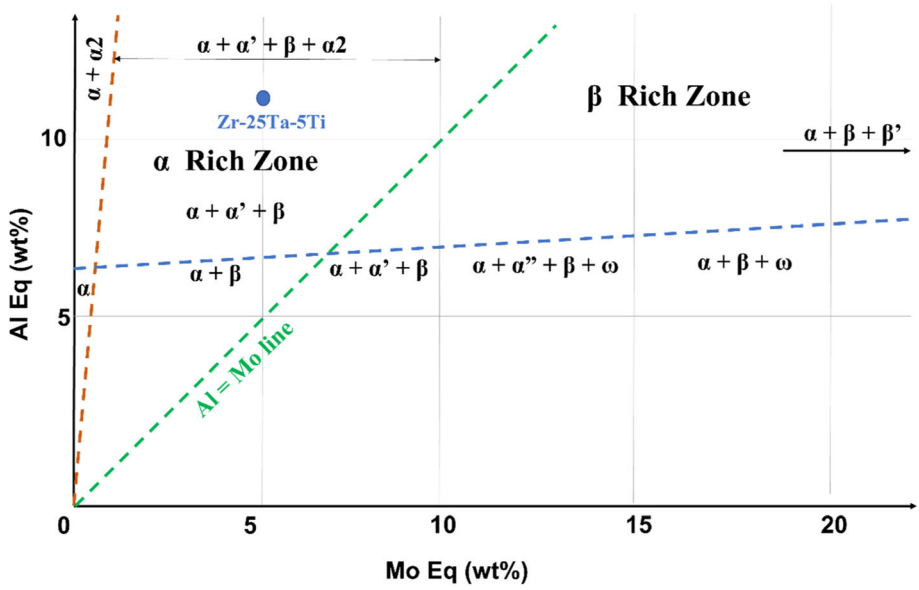

Fig. 3 Plot of Al equivalency (Al-eq) and Mo equivalency (Mo-eq) for titanium alloys (adapted from John Mantione et al. 2020 (Ref 35))

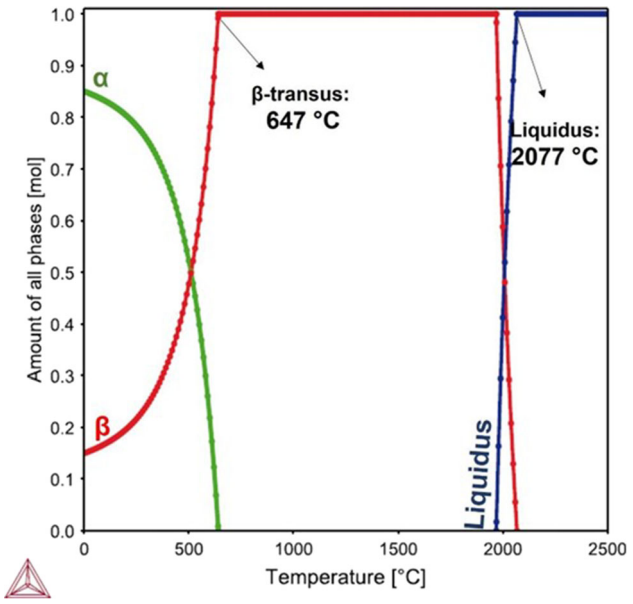

Fig. 4 Plot of Zr-25Ta-5Ti in Thermo-Calc simulation (SGTE PURE5 database)

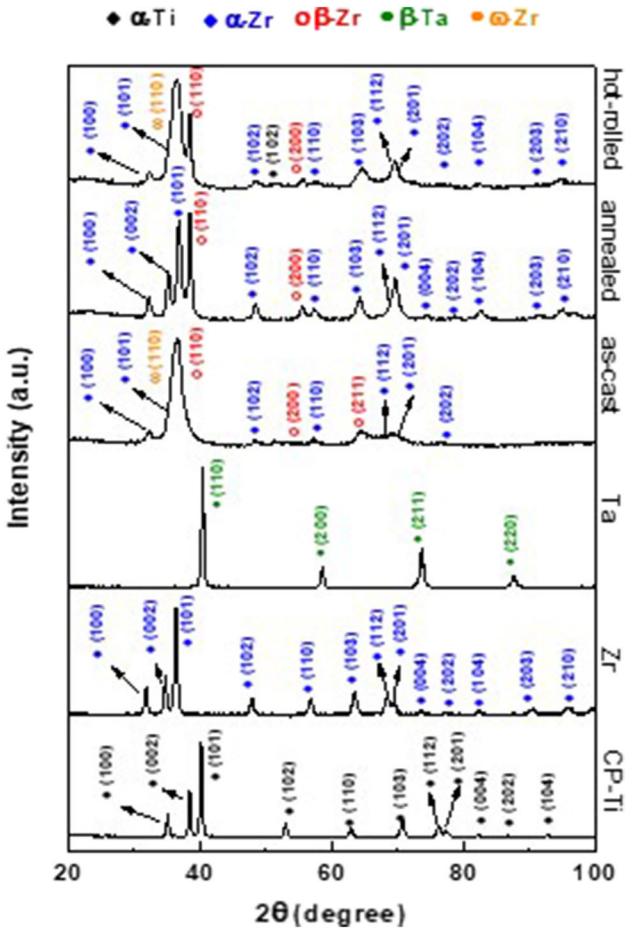

Fig. 5 X-ray diffraction patterns for pure elements (Ti, Zr and Ta) and Zr-25Ta-5Ti in all studied conditions

(α phase), body-centered cubic (β phase), and tetragonal crystal structure (ω phase). Due to the presence of the ω phase, this alloy should have high hardness and elastic modulus values, making it unsuitable for biomedical applications after melting (Ref 37).

After the annealing treatment, the alloy exhibits only peaks corresponding to the α and β phases. In contrast, the previously observed ω phase has been suppressed due to the emergence of additional α phase peaks. This suppression can be attributed to titanium in the alloy, which acts as an α-stabilizing element (Ref 38). The incorporation of titanium contributes to the high values of elastic modulus and hardness, thereby facilitating the potential use of the alloy as a bone substitute in future applications (Ref 2). It is worth mentioning that the slow cooling during the annealing process provides favorable thermodynamic conductions for forming stable Zr phases at low temperatures, in this case, the α phase.

Finally, after hot-rolling in the alloy, the α and β phases peaks are maintained, and the ω phase reappears due to the high-temperature rolling (Ref 39). The structure of the as-cast and hot-rolled conditions is very similar.

The micrographs obtained by scanning electron microscopy are shown in Fig. 6. The as-cast condition alloy presents grain contours, the characteristic microstructure of the β phase, as it can be observed that only 25% of Tantalum is enough to maintain the β phase. In the micrographs, it is impossible to see the α phase, characterized by intra-grain needles, although it has already been observed on XRD (Ref 31).

The annealed alloy shows some agglomerates composed of Ta, as shown in the micrograph in Fig. 6. The agglomeration is due to the high-temperature treatment and the lower diffusivity of tantalum compared to other elements present. Additionally, the micrograph reveals grain boundaries, β phase, and intra-grain needles characteristic of alloys with the α phase.

Finally, the hot-rolled alloy's micrograph presents the same agglomerates previously seen in the annealed ones, but in smaller quantities, in addition to grain boundaries characteristic of the β phase and intra-grain needles characteristic alloys with the α phase. The XRD analysis corroborates these results, it is important to note that the ω phase can be detected through transmission electron microscopy (Ref 40).

The Mo and Al theory, as shown in Fig. 3, predicted that the alloy would be rich in the α phase. However, after x-ray diffraction analysis and optical microscopy, it was observed that this theory did not apply to the studied alloy. In optical microscopy, characteristic microstructures of the β phase were identified, while x-ray diffraction revealed peaks corresponding to the α, β, and ω phases. These results indicate that the Zr-25Ta-5Ti alloy exhibits a complex phase distribution beyond the initial theoretical prediction based solely on the Mo and Al parameters.

In addition, the results of structural and microstructural characterization indicated that the annealed condition has a greater amount of α phase; due to this behavior, it is understood why the annealed alloy has a higher density value than the other conditions (as-cast and e hot-rolled). The α phase is responsible for increasing the density in the annealed condition, as the compact hexagonal phase has a higher atomic packing factor compared to the body-centered cubic crystalline structure.

Two mechanical properties tests were carried out to determine the hardness and elastic modulus of the alloy (Table 1). Understanding the hardness of biomedical alloys is crucial because metals with high hardness are usually brittle, making it difficult for mechanical forming to produce biomedical rods, plates, and screws (Ref 41). The as-cast condition

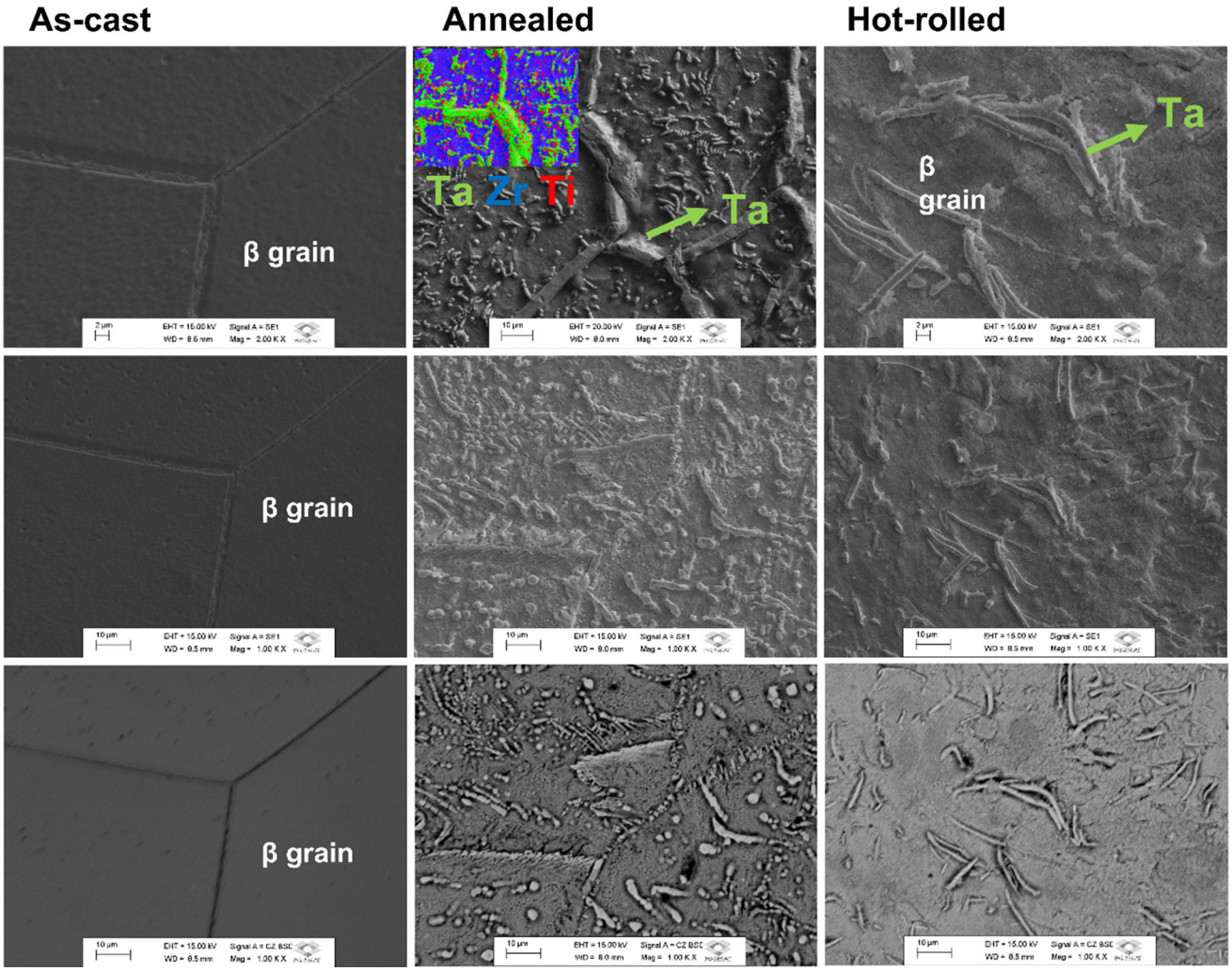

Fig. 6 Scanning electron microscopy images for Zr-25Ta-5Ti

Table 1 Vickers microhardness and elastic modulus of the as-cast, annealed, and hot-rolled Zr-25-5Ti alloy

Alloys	Microhardness (HV)	Elastic Modulus (GPa)
Zr-25Ta-5Ti (as-cast)	499 ± 5	88 ± 5
Zr-25Ta-5Ti (annealed)	272 ± 8	112 ± 7
Zr-25Ta-5Ti (hot-rolled)	382 ± 7	86 ± 5

alloy has a hardness value of approximately 500 HV, higher than the CP-Zr element (150 HV). With the annealing process, the hardness value of the alloy dropped by almost half, to 272 HV, making the alloy viable for applications as a biomaterial. The Zr-25Ta-5Ti after the hot-rolling has had an increased hardness value compared to the annealed sample at 382 HV.

The analysis of hardness values provides valuable insights into the effects of the annealing process on the alloy. The annealing treatment resulted in a reduction in the hardness of the alloy under the investigated conditions. The decrement in hardness can be attributed to eliminating the ω phase from the alloy's microstructure following the annealing process, as confirmed by the x-ray diffraction analysis. Conversely, the alloy subjected to the rolling process exhibited a notable increase in hardness compared to the annealed counterpart. The increase can be attributed to the reoccurrence of the ω phase within the alloy's microstructure, known for its inherent high hardness properties. These findings highlight the significant influence of phase transformations on the mechanical properties of the Zr-25Ta-5Ti alloy and emphasize the potential for tailoring its hardness through appropriate thermal treatments.

Regarding elastic modulus, it can be observed that the value of the elastic modulus for the annealed alloy is very high when considering its use as a biomaterial. However, after hot-rolling, it is possible to observe a decrease in the value, making the alloy promising for use as a biomaterial, especially when compared to CP-Zr. This increase is probably associated with the ω phase. Concerning the elastic modulus, high values of elastic modulus are undesirable. Thus, the alloy after rolling has a better result than many orthopedic and dental implant alloys, such as CP-Ti, CP-Ta, Ti-6Al-4 V, Ti-15Mo, Co-Cr alloys, and stainless steel (Ref 6).

Wear analyzes were performed on the Zr-25Ta-5Ti alloy in all conditions studied (as-cast, annealed, and hot-rolled) using the ball cratering technique. For a simple comparison, the surfaces of CP-Ti and commercial Ti-6Al-4 V alloy were ground. Figure 7 shows the craters produced on the surfaces of materials a), along with wear volume and wear coefficient data b).

Crater images show that the Zr-25Ta-5Ti alloy has a worse resistance to abrasive wear compared to CP-Ti and Ti-6Al-4 V, mainly for the alloy in the hot-rolled condition that has the highest value of worn volume (0.5 mm^3), consequently, a higher wear coefficient value (K = 6 x 10^{-10} mm^3/N.mm).

As previously noted, the structural and microstructural characterization analyses showed that the Zr-25Ta-5Ti alloy has the ω phase in its crystalline phase. Numerous studies in the literature report the effect of the ω phase on changing the mechanical properties and hardness of titanium and zirconium alloys intended for biomedical applications, showing that this phase is undesirable for metals used in orthopedics and dentistry due to its hardening and weakening effect. (Ref 38, 42, 43). Due to the ω phase, the alloys produced in this work do not have good wear resistance results.

Due to low wear resistance, the Zr-25Ta-5Ti alloy does not have a high potential for use as load-bearing implants or joint implants (hip and knee). Even so, the material can be used in regions of the human body where the bone is not subject to mechanical stress, such as the skull, or as a fixation prosthesis, screws, scalpels, and other medical devices that have short contact with the human body.

Finally, a classical cytotoxicity assay was applied in order to better know whether this biomaterial prototype triggered some toxicity considering osteoblasts. The data from MTT assay show there is no cytotoxicity effect in osteoblasts, once Fig. 8a brings a very similar performance of cells responding to both control and Zr-25Ta-5Ti. Important to mention that in accordance to ISO10993 standard (Ref 44), a percentage difference in cell absorbance greater than 70% compared to the control group is required for considering a material being cytotoxic. This strategy of measuring cytotoxicity of biomaterials using MTT has longer been used (Ref 45). Thereafter, a better comprehension of the effect of the Zr-25Ta-5Ti on osteoblast adhesion was also concerned in study. Figure 8b shows there is no difference between control and Zr-25Ta-5Ti, and it means a high capacity of the material in promoting cell adhesion, once polystyrene has been used as control in this experiment and polystyrene is widely used as polymer in cell culture staffs. Altogether, the data show there is non-cytotoxic effect. Therefore, the alloy demonstrated primary potential for use as a biomaterial (Ref 25). Thus, this data gathers enough evidence that Zr-25Ta-5Ti does not trigger any deleterious effect in osteoblast, and studies are called for better understating its effect on osteoblast metabolism (Ref 46).

4. Conclusion

Considering that: (i) The chemical composition analysis and EDS mapping indicate that the alloy maintained the stoichiometry proposed in this work; (ii) The density values indicate that the stoichiometry of the alloy was respected and that this value tends to increase after annealing heat treatment due to the α phase form; (iii) The as-cast alloy condition predominates the β phase, with the coexistence of α and ω phases. The micrographs show equiaxed grain structures characteristic of the β phase; (iv) After annealing heat treatment, the ω phase was suppressed, and the α phase appeared. The micrographs show equiaxed grain structures, characteristic of the β phase, and needle-like lamellar structures, characteristic of the α phase; (v) After hot-rolling, the alloy maintains the predominance of the α

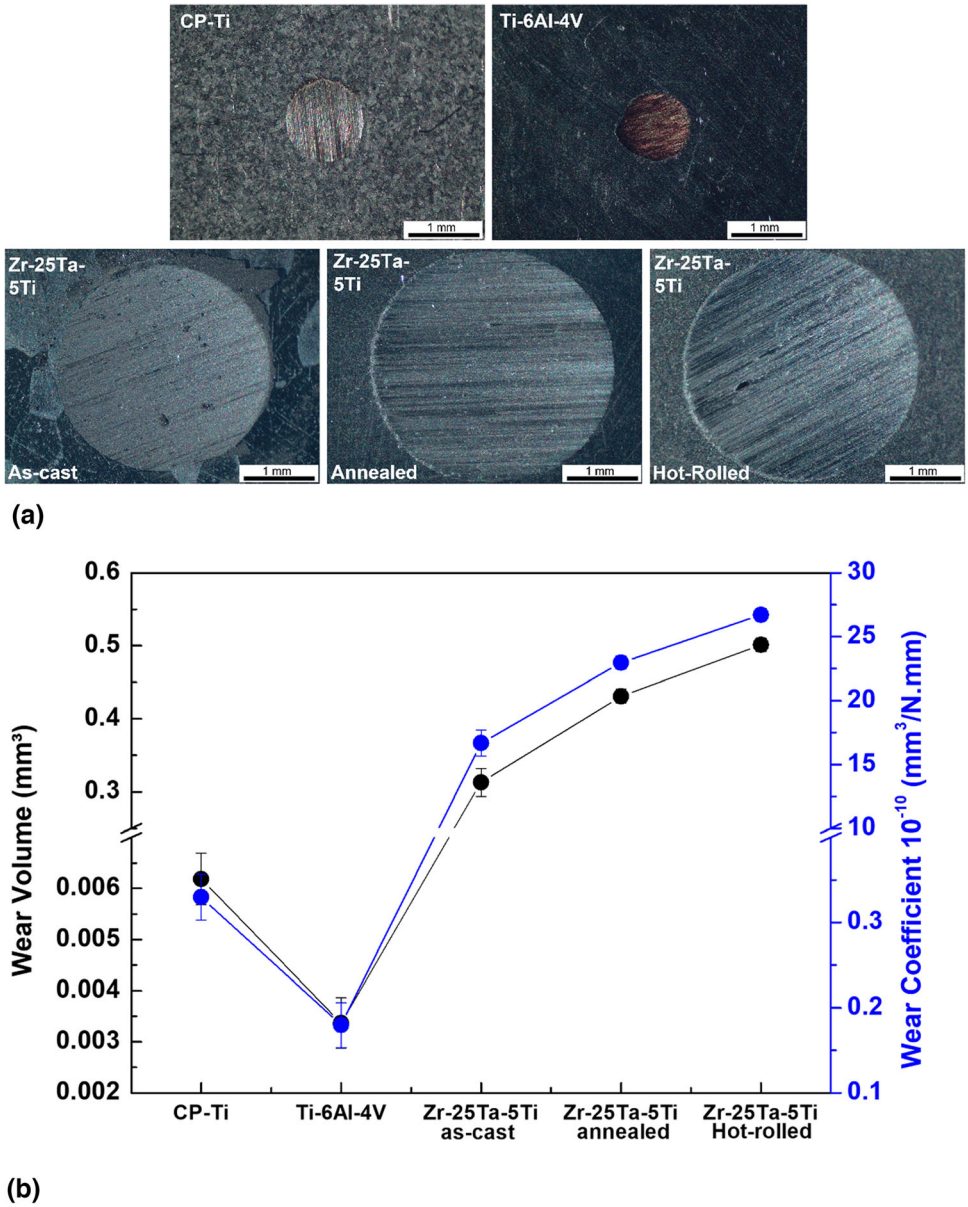

Fig. 7 Image of the characteristic craters of samples worn by the ball cratering technique carried out on the surface of CP-Ti, Ti-6Al-4 V, and Zr-25ta-5Ti alloys (a), in addition to the values of the worn value and coefficient of wear obtained through the tests (b)

phase and the coexistence of the β and ω phases; (vi) The microhardness test shows that the as-cast alloy is not viable for use as a biomaterial due to its high hardness, justified by the presence of the ω phase. However, the values tend to decrease with heat treatment and hot-rolling; (vii) The elastic modulus of the Zr-25Ta-5Ti alloy tends to decrease with the hot-rolling process, which is a good value and better than many orthopedic and dental implant alloys such as CP-Ti, CP-Ta, Ti-6Al-4 V, Ti-15Mo, Co-Cr alloys, and stainless steel; (viii) The wear tests showed that the Zr-25Ta-5Ti alloy has a low resistance to abrasive wear. This behavior is due to the formation of the ω phase, which has the characteristic of weakening the alloy; (ix) CP-Ti and Ti-6Al-4 V alloys have higher wear resistance compared to Zr-25Ta-5Ti zirconium alloy; and (x) Zr-25Ta-5Ti alloy provides preliminary information on biocompatibility. Altogether, the data shown in this study reinforce the possibility of the Zr-25Ta-5Ti alloy in being considered for biomedical applications; however, a set of methodological strategies still needs to be considered in order to better investigate the lack when the biological responses are considered at this stage of development of biomaterials.

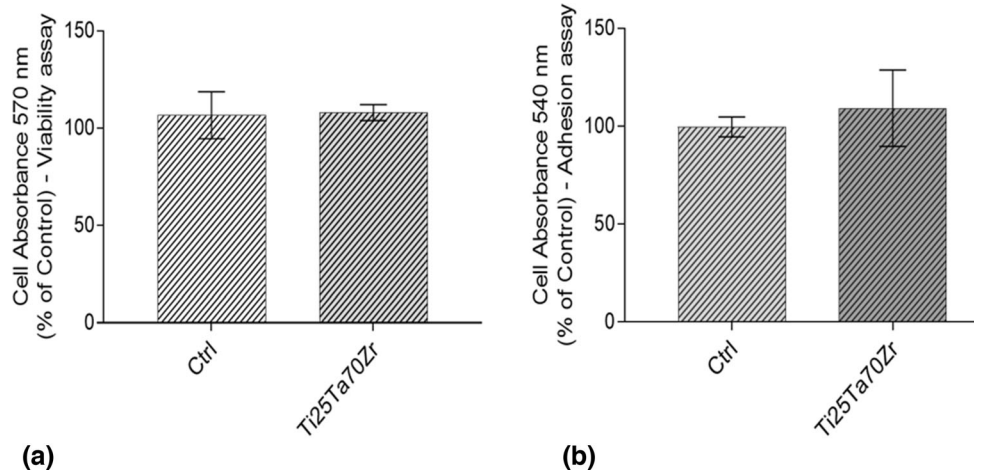

Fig. 8 (a) Cellular Viability Test and (b) Cellular Adhesion Test for the Zr-25Ta-5Ti alloy after annealing heat treatment

Acknowledgments

The authors would like to thank the Faculdade de Ciências de Bauru for the ease of SEM measurements, Professor Fenelon Martinho Lima Pontes for the XRD measurements, and would thank Brazilian agencies CAPES Finance Code 001, CAPES grant # 88881.310568/2018-01, CNPq grant # 314.810/2021-8, and FAPEP grant # 2019/26517-6 for their financial support.

Author's Contributions

Edriely de Oliveira Saraiva was involved in data collection, data analysis/interpretation, and writing. Dr. Pedro Akira Bazaglia Kuroda contributed to data collection, data analysis/interpretation, and writing. Dr. Gerson Santos de Almeida was involved in data collection and data analysis/interpretation. Dr. Willian Fernando Zambuzzi contributed to data analysis/interpretation and critical revision of article. Dr. Carlos Roberto Grandini was involved in concept/design and critical revision of article.

Conflict of interest

The authors declare that they have no conflicts of interest with the contents of this article.

References

1. K. Prasad, O. Bazaka, M. Chua, M. Rochford, L. Fedrick, J. Spoor, R. Symes, M. Tieppo, C. Collins, and A. Cao, Metallic Biomaterials: Current Challenges and Opportunities, *Materials*, 2017, **10**(8), p 884.
2. S.S. Sidhu, H. Singh, and M.A.-H. Gepreel, A Review on Alloy Design, Biological Response, and Strengthening of β-Titanium Alloys as Biomaterials, *Mater. Sci. Eng. C*, 2021, **121**, p 111661.
3. I. Putrantyo, N. Anilbhai, R. Vanjani, and B. De Vega, Tantalum as a Novel Biomaterial for Bone Implant: A Literature Review, *J. Biomim. Biomater. Biomed. Eng.*, 2021, **52**, p 55–65.
4. M. Navarro, A. Michiardi, O. Castano, and J.A. Planell, Biomaterials in Orthopaedics, *J. Royal Soc. Interface Royal Soc.*, 2008, **5**(27), p 1137–1158.
5. A. International, R.J. Narayan, Materials for medical devices, ASM international, 2012
6. M. Geetha, A.K. Singh, R. Asokamani, and A.K. Gogia, Ti Based Biomaterials, the Ultimate Choice for Orthopaedic Implants–A Review, *Prog. Mater Sci.*, 2009, **54**(3), p 397–425.
7. M. Kaur and K. Singh, Review on Titanium and Titanium Based Alloys as Biomaterials for Orthopaedic Applications, *Mater. Sci. Eng., C*, 2019, **102**, p 844–862.
8. B.R. Martins, T.S. Pinto, C.J. da Costa Fernandes, F. Bezerra, and W.F. Zambuzzi, PI3K/AKT Signaling Drives Titanium-Induced Angiogenic Stimulus, *J. Mater. Sci. Mater. Med.*, 2021, **32**(1), p 18.
9. R.P. Kolli and A. Devaraj, A Review of Metastable beta Titanium Alloys, *Metals*, 2018, **8**(7), p 506.
10. A. ASTM, C150/C150M-17, standard specification for Portland cement, *Am. Soc. Test. Mater. West Conshohocken, PA, USA*, (2017)
11. C.F.C.J. da Célio, R.A. da Silva, P. Fretes Wood, S.A. Teixeira, F. Bezerra, and W.F. Zambuzzi, The Molecular Pathway Triggered by Zirconia in Endothelial Cells Involves Epigenetic Control, *Tissue & Cell*, 2021, **73**, p 101627.
12. C.J. da Costa Fernandes, M.R. Ferreira, F.J.B. Bezerra, and W.F. Zambuzzi, Zirconia Stimulates ECM-Remodeling as a Prerequisite to Pre-Osteoblast Adhesion/Proliferation by Possible Interference with Cellular Anchorage, *J. Mater. Sci. Mater. Med.*, 2018, **29**(4), p 41.
13. L. Saldaña, A. Mendez-Vilas, L. Jiang, M. Multigner, J.L. Gonzalez-Carrasco, M.T. Perez-Prado, M.L. Gonzalez-Martin, L. Munuera, and N. Vilaboa, In Vitro Biocompatibility of an Ultrafine Grained Zirconium, *Biomaterials*, 2007, **28**(30), p 4343–4354.
14. P. Ji, S. Liu, C. Shi, K. Xu, Z. Wang, B. Chen, B. Li, Y. Yang, and R. Liu, Synergistic Effect of Zr Addition and Grain Refinement on Corrosion Resistance and Pitting Corrosion Behavior of Single α-Phase Ti-Zr-Based Alloys, *J. Alloy. Compd.*, 2022, **896**, p 163013.
15. B.R. Levine, S. Sporer, R.A. Poggie, C.J. Della Valle, and J.J. Jacobs, Experimental and Clinical Performance of Porous Tantalum in Orthopedic Surgery, *Biomaterials*, 2006, **27**(27), p 4671–4681.
16. A. Standard, E407: ASTM International: West Conshohocken, ed., PA, (2007)
17. P.A.B. Kuroda, R.F.M. dos Santos, C.R. Grandini, and C.R.M. Afonso, Unveiling the Effect of Nb and Zr Additions on Microstructure and Properties of β Ti-25Ta Alloys for Biomedical Applications, *Mater. Charact.*, 2024, **207**, p 113577.
18. P.A.B. Kuroda, R.F.M. dos Santos, M.C. Rossi, D.R.N. Correa, C.R. Grandini, and C.R.M. Afonso, Influence of Zr Addition in β Ti-25Ta-xZr Alloys on Oxide Formation by MAO-Treatment, *Vacuum*, 2023, **217**, p 112541.
19. A.d. E1876-15, "Standard Test Method for Dynamic Young's Modulus, Shear Modulus, and Poisson's Ratio by Impulse Excitation of Vibration," ASTM International 2015
20. D. Sánchez-Huerta, N. López-Perrusquia, E. García, I. Hilerio-Cruz, M. Flores-Martínez, M.A. Doñu-Ruiz, and S. Muhl, Micro-Abrasive Wear Behavior by the Ball Cratering Technique on AISI L6 Steel for Agricultural Application, *Mater. Lett.*, 2021, **283**, p 128904.
21. P.A.B. Kuroda, F.N. de Mattos, C.R. Grandini, and C.R.M. Afonso, Micro-Abrasive Wear Behavior by Ball Cratering on MAO Coating of Ti-25Ta Alloy, *J. Mater. Res. Technol.*, 2023, **26**, p 1850.
22. C.J. da Costa Fernandes, F.J.B. Bezerra, B. de Campos Souza, M.A. Campos, and W.F. Zambuzzi, Titanium-Enriched Medium Drives Low

Profile of ECM Remodeling as a Pre-Requisite to Pre-Osteoblast Viability and Proliferative Phenotype, *J. Trace Elem. in Med. Biol. Organ Soc. Miner. Trace Elements (GMS)*, 2018, **50**, p 339–346.
23. W.F. Zambuzzi, E.A. Bonfante, R. Jimbo, M. Hayashi, M. Andersson, G. Alves, E.R. Takamori, P.J. Beltrão, P.G. Coelho, and J.M. Granjeiro, Nanometer Scale Titanium Surface Texturing Are Detected by Signaling Pathways Involving Transient FAK and Src Activations, *PLoS ONE*, 2014, **9**(7), p e95662.
24. R.A. da Silva, G. da Silva Feltran, M.R. Ferreira, P.F. Wood, F. Bezerra, and W.F. Zambuzzi, The Impact of Bioactive Surfaces in the Early Stages of Osseointegration: An In Vitro Comparative Study Evaluating the HAnano® and SLActive® Super Hydrophilic Surfaces, *Biomed. Res. Int.*, 2020, **2020**, p 3026893.
25. G.C. Cardoso, G.S. de Almeida, D.O.G. Corrêa, W.F. Zambuzzi, M.A.R. Buzalaf, D.R.N. Correa, and C.R. Grandini, Preparation and Characterization of Novel as-cast Ti-Mo-Nb Alloys for Biomedical Applications, *Sci. Rep.*, 2022, **12**(1), p 11874.
26. D.R.N. Correa, P.A.B. Kuroda, M.L. Lourenço, C.J.C. Fernandes, M.A.R. Buzalaf, W.F. Zambuzzi, and C.R. Grandini, Development of Ti-15Zr-Mo Alloys for Applying as Implantable Biomedical Devices, *J. Alloy. Compd.*, 2018, **749**, p 163–171.
27. A.d. F2066-13, "Standard Specification for Wrought Titanium-15 Molybdenum Alloy for Surgical Implant Applications (UNS R58150)," p 6 2013
28. S. Zhu, C. Zhu, D. Luo, X. Zhang, and K. Zhou, Development of a Low-Density and High-Strength Titanium Alloy, *Metals*, 2023, **13**(2), p 251.
29. M.R. Rahimzadeh, M.R. Rahimzadeh, S. Kazemi, R.J. Amiri, M. Pirzadeh, and A.A. Moghadamnia, Aluminum Poisoning with Emphasis on Its Mechanism and Treatment of Intoxication, *Emerg. Med. Int.*, 2022, **2022**, p 1480553.
30. G.C. Cardoso, M.A.R. Buzalaf, D.R.N. Correa, and C.R. Grandini, Effect of Thermomechanical Treatments on Microstructure, Phase Composition, Vickers Microhardness, and Young’s Modulus of Ti-xNb-5Mo Alloys for Biomedical Applications, *Metals*, 2022, **12**(5), p 788.
31. G.C. Cardoso, P.A.B. Kuroda, and C.R. Grandini, Influence of Nb Addition on the Structure, Microstructure, Vickers Microhardness, and Young's Modulus of New β Ti-xNb-5Mo Alloys System, *J. Mater. Res. Technol.*, 2023, **25**, p 3061–3070.
32. M.C. Lucchetti, G. Fratto, F. Valeriani, E. De Vittori, S. Giampaoli, P. Papetti, V. Romano Spica, and L. Manzon, Cobalt-Chromium Alloys in Dentistry: An Evaluation of Metal Ion Release, *J. Prosthetic Dent.*, 2015, **114**(4), p 602–608.
33. Y. Guo, J. Niu, J. Cao, Z. Sun, Z. Dan, and H. Chang, Relative Strength of β Phase Stabilization by Transition Metals in Titanium Alloys: The Mo Equivalent from a first Principles Study, *Mater. Today Commun.*, 2023, **35**, p 106123.
34. A. Mehjabeen, W. Xu, D. Qiu, and M. Qian, Redefining the β-Phase Stability in Ti-Nb-Zr Alloys for Alloy Design and Microstructural Prediction, *JOM*, 2018, **70**(10), p 2254–2259.
35. J. Mantione, M. Garcia-Avila, M. Arnold, D. Bryan, and J. Foltz, Properties of Novel High Temperature Titanium Alloys for Aerospace Applications, *MATEC Web Conf.*, 2020, **321**, p 04006.
36. H. Chen and T. Barman, Thermo-Calc and DICTRA Modelling of the β-Phase Depletion Behaviour in CoNiCrAlY Coating Alloys at Different Al Contents, *Comput. Mater. Sci.*, 2018, **147**, p 103–114.
37. M. Li and X. Min, Origin of ω-Phase Formation in Metastable β-type Ti-Mo Alloys: Cluster Structure and Stacking Fault, *Sci. Rep.*, 2020, **10**(1), p 8664.
38. P.A.B. Kuroda, B.L.T. Pedroso, F.M.L. Pontes, and C.R. Grandini, Effect of Titanium Addition on the Structure, Microstructure, and Selected Mechanical Properties of As-Cast Zr-25Ta-xTi Alloys, *Metals*, 2021, **11**(10), p 1507.
39. W.-F. Ho, W.-K. Chen, S.-C. Wu, and H.-C. Hsu, Structure, Mechanical Properties, and Grindability of Dental Ti–Zr Alloys, *J. Mater. Sci. Mater. Med.*, 2008, **19**(10), p 3179–3186.
40. G. Alphy, V. Sharma, R. Divakar, M. Sabeena, and E. Mohandas, Transmission Electron Microscopy Studies and Modeling of 3D Reciprocal Space of ω Forming Alloy, *Micron*, 2017, **102**, p 73–87.
41. P.A.B. Kuroda, F.D.F. Quadros, R.O.D. Araújo, C.R.M. Afonso, and C.R. Grandini, Effect of Thermomechanical Treatments on the Phases, Microstructure, Microhardness and Young's Modulus of Ti-25Ta-Zr Alloys, *Materials*, 2019, **12**(19), p 3210.
42. A.S. Gornakova, A. Korneva, A.I. Tyurin, N.S. Afonikova, A.R. Kilmametov, and B.B. Straumal, Omega Phase Formation and Mechanical Properties of Ti–15 wt.% Mo and Ti–1.5 wt.% Mo Alloys after High-Pressure Torsion, *Processes*, 2023, **11**(1), p 221.
43. G.C. Cardoso, P.A.B. Kuroda, and C.R. Grandini, Influence of Nb Addition on the Structure, Microstructure, Vickers Microhardness, and Young's Modulus of New β Ti-xNb-5Mo Alloys System, *J. Market. Res.*, 2023, **25**, p 3061–3070.
44. I. 10993, "Biological evaluation of medical devices.," 2005
45. S. Bertazzo, W.F. Zambuzzi, D.D. Campos, C.V. Ferreira, and C.A. Bertran, A Simple Method for Enhancing Cell Adhesion to Hydroxyapatite Surface, *Clin. Oral Implants Res.*, 2010, **21**(12), p 1411–1413.
46. S. Gemini-Piperni, E.R. Takamori, S.C. Sartoretto, K.B. Paiva, J.M. Granjeiro, R.C. de Oliveira, and W.F. Zambuzzi, Cellular Behavior as a Dynamic Field for Exploring Bone Bioengineering: A Closer Look at Cell-Biomaterial Interface, *Arch. Biochem. Biophys.*, 2014, **561**, p 88–98. (**(in eng)**)